

E. SCHAFLER* **, L. TARKOWSKI***, J. BONARSKI***, I. KOPACZ*, R. PIPPAN* ****,
H.P. STÜWE*

**TEXTURE EVOLUTION AND MICROSTRUCTURE OF ECAP Cu DETERMINED BY
XRD AND EBSD**

**ROZWÓJ TEKSTURY I MIKROSTRUKTURY W Cu PO PROCESIE ECAP
OKREŚLONEJ TECHNIKAMI DYFRAKЦИИ RENTGENOWSKIEJ ORAZ EBSD**

The equal channel angular pressing (ECAP) as a method of severe plastic deformation imposes high strains to the materials deformed. The consequence is the crystal fragmentation of the material leading to an ultrafine or even nanograined structure yielding various improved properties. Since ECAP can achieve extraordinarily high plastic strain of material, the evolution of crystallographic texture, misorientation distribution and crystal size are of high interest. These properties have been investigated for the example of room temperature deformation by ECAP under variation of pass number (up to 16) as well as route type (A, B_C and C). Based on the orientation distribution function (ODF) in the Euler angles space, the development of texture and periodical changes of its main components has been analyzed. The evolution of misorientation of the deformed microstructure accompanied with its fragmentation was observed by electron back scatter diffraction (EBSD) in terms of changeable parameters of deformation. The obtained orientation maps also reflect the influence of the macroscopic shear conditions on the development of microstructure.

Metoda silnej deformacji plastycznej ECAP (equal channel angular pressing) pozwala osiągnąć bardzo duże odkształcenie materiału. Konsekwencją zastosowania takiego sposobu odkształcenia jest fragmentacja krystalitów prowadząca do struktury ultradrobnoziarnistej lub nanokrystalicznej poprawiającej znacznie właściwości mechaniczne materiału.

Z uwagi na szczególnie silne odkształcenie plastyczne materiału, interesujący staje się rozwój tekstury krystalograficznej, rozkład wzajemnych dezorientacji krystalitów jak i ich rozmiar. Parametry te były badane na przykładzie próbek Cu odkształconych metodą ECAP w temperaturze pokojowej. Zastosowano różną liczbę przepustów (maksymalnie 16) według drogi A, B_C i C. Na podstawie funkcji rozkładu orientacji (FRO) przeanalizowano rozwój

* WRICH SCHMID INSTITUTE OF MATERIALS SCIENCE, AUSTRIAN ACADEMY OF SCIENCES, A-8700 LEOBEN, AUSTRIA

** INSTITUTE OF MATERIALS PHYSICS, UNIVERSITY OF VIENNA, A-1090 WIEN, AUSTRIA

*** INSTYTUT METALURGII I INŻYNIERII MATERIAŁOWEJ IM. A. KRUPKOWSKIEGO, POLSKA AKADEMIA NAUK, 30-059 KRAKÓW, UL. REYMONTA 25

**** CHRISTIAN DOPPLER LABORATORY OF LOCAL ANALYSIS OF DEFORMATION AND FRACTURE, A-8700 LEOBEN, AUSTRIA

tekstury i periodyczne zmiany jej głównych składowych. Zmiany w rozkładzie dezorientacji i mikrostrukturze towarzyszące fragmentacji krystalitów były obserwowane techniką EBSD w zależności od parametrów deformacji. Uzyskane mapy orientacji odzwierciedlają również wpływ makroskopowych warunków ścinania na mikrostrukturę odkształcanej miedzi.

1. Introduction

Equal channel angular pressing (ECAP) has been established as one of the methods of severe plastic deformation, which offer the possibility to reach highest strains by application to metals, alloys and composites [1]. Reinserting the specimen several times into a tool consisting of two channels with equal diameter, which intersect at an angle ϕ , provides straining without change of sample shape and destruction. This offers a procedure to produce ultra-fine grained materials with significantly changed physical properties (mechanical, electrical and magnetic) [2].

In order to enable strain path changes, the sample can be rotated around the channel axis between two successive pressings (passes). For this purpose a notation system has been introduced [3, 4]: routes *A*, *B* and *C* correspond to rotations of 0° , 90° and 180° , respectively. Route *B* can be distinguished in B_A and B_C , for the rotation direction changed after each pass and consecutive rotation in the same direction, respectively.

There are several publications reporting the texture of ECAP-deformed materials: Al, Be, Cu, Fe, Mg, Ni, Ti [5-17]; most of these are focusing on results from tools with a die angle equal to 90° . In this work the texture and microstructure investigation are presented for Cu during ECAP-deformation with a 120° die angle tool using route *A*, B_C and *C*. This has been performed by means of two techniques: X-ray diffraction and electron back scatter diffraction (EBSD).

2. Experimental details

The die for ECAP used in the present work had a square cross section with dimensions of $15 \times 15 \text{ mm}^2$ and a die angle equal to 120° . For processing, copper samples were machined with dimensions of $35 \times 15 \times 15 \text{ mm}$ and annealed at 650°C for 2 hours. The unequal extents of deformation (= number of passes) of the different routes result from the evolution of the macroscopic shape of the samples and possible initial sample length (due to the tool). After each pass the geometry of the samples subjected to route *A* and *B* has to be corrected in order to comply ideal load transmission from the plunger to the sample. For this reason the samples become shorter with each pass and are limited to a certain number of passes, otherwise the material will get very inhomogeneous [18].

For the standard texture measurements the samples were cut out by means of a wire machine in the central part of the ingot at a plane containing the extrusion direction "ED" and the transverse direction "TD" (see Fig. 6). After the cutting, about 2 mm thick surface layer of each sample has been removed by grinding then it was

mechanically polished and finally etched. The texture was examined by registering (111), (200) (220), and (311) pole figures using filtered X-ray beam of $\text{CuK}\alpha$ series. Based on the incomplete pole figures, corrected for defocussation and background, the volume fractions of main texture components have been calculated by integrating the counts within $\pm 5^\circ$ tolerance to the ideal orientation of the component. This has been performed using LABOSOFT-“LaboTex” software.

Texture of the same samples has been investigated by the EBSD technique using a LEICA Stereoscan 440. Before, the sample surfaces were additionally electropolished. However, in the case of EBSD, the measurement sample areas were considerably smaller than in case of the X-ray diffraction. The evaluation of the grain size distribution was performed with orientation imaging microscopy (OIM) software.

3. Results

In Fig. 1, the texture after 1st ECAP pass is represented by the (111) pole figure determined by standard X-ray texture measurement, whereas the three identified texture components are indicated in the separate presentations of the pole figure.

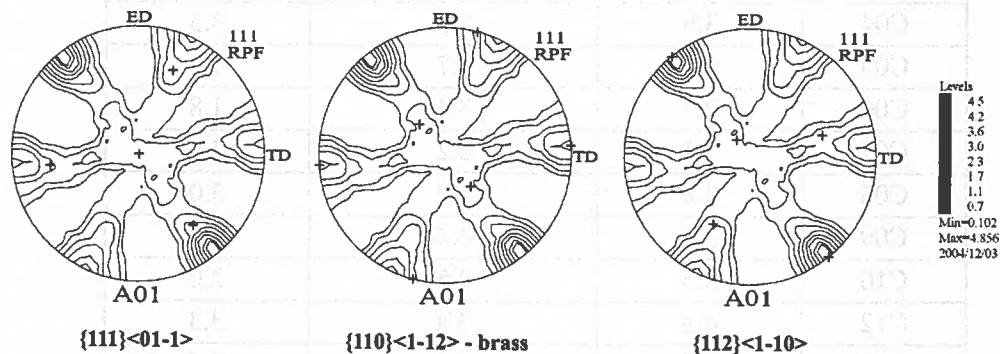


Fig. 1. The percentage of the volume fractions of the identified (indicated) texture components for deformation route A, B and C, determined by quantitative analysis of the orientation distribution

In Figs. 2 - 4 the texture evolution of the continued deformation is presented by the (111) pole figures for routes A, B and C, respectively.

TABLE

The percentage of the volume fraction of the identified (indicated) texture components for deformation route A, B and C, determined by quantitative analysis of the orientation distribution

Sample	(111)[01 $\bar{1}$]	(110)[1 $\bar{1}$ 2](Brass)	(112)[1 $\bar{1}$ 0]
1 pass	5.3	4.7	3.3
A02	7.4	2.8	3.1
A03	5.5	1.3	2.5
A04	5.1	1.1	1.8
A05	5.3	1.4	1.5
A06	8.2	2.7	2.4
A07	6.8	1.9	2.3
B02	10.7	0.7	5.8
B03	6.5	0.6	4.2
B04	3.8	0.6	3.4
B05	4.3	0.7	3.3
C02	2.3	3.5	2.2
C03	3.9	4.0	2.9
C04	3.9	2.5	3.3
C05	5.7	5.7	4.3
C06	2.7	3.4	1.8
C07	5.1	6.2	3.6
C08	3.8	3.9	3.0
C09	3.8	3.4	2.7
C10	3.5	3.5	2.0
C12	4.5	3.4	3.3
C14	3.4	3.6	2.6
C16	6.0	5.8	4.8

Table 1 presents the calculated volume fractions of the three main texture components for all three deformation routes.

Fig. 5 shows the orientation maps determined by electron back scatter diffraction after 2nd ECAP passes deformed by route A and C, respectively. In all maps the colour designates the orientation with respect to the surface normal direction according to

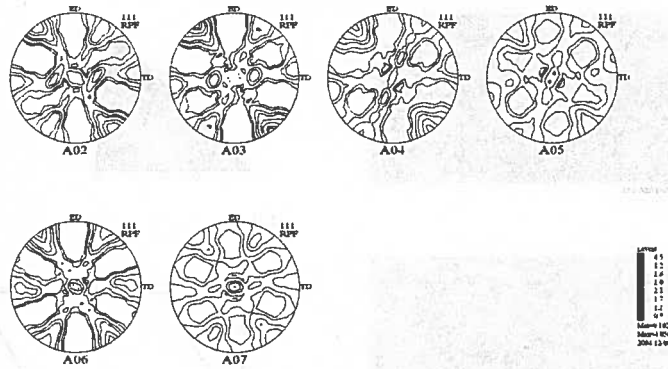


Fig. 2. the recalculated (111) pole figures of ECAP-Cu for 2 — 7 passes of route A deformation

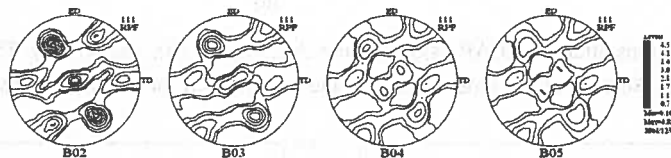


Fig. 3. The recalculated (111) pole figures of ECAP-Cu for 2 — 5 passes of route B deformation

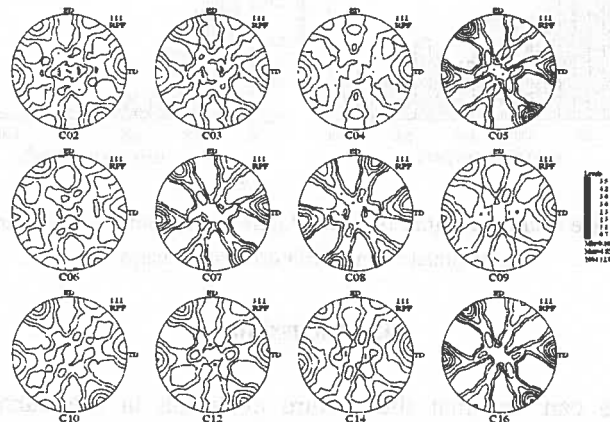


Fig. 4. The recalculated (111) pole figure of ECAP-Cu for 2 — 16 passes of route C deformation

the colour key of the unit triangle of standard stereographic projection (Fig. 5c). All patterns were subjected to a cleaning procedure in order to remove points of the frame, which cannot be evaluated by the OIM system software.

The grain size distribution has been evaluated from the EBSD orientation maps. Within a misorientation angle of 10 degrees two adjacent point were considered to belong to the same grain. The distributions for 1 pass and 4 passes in route C are shown in Fig.6.

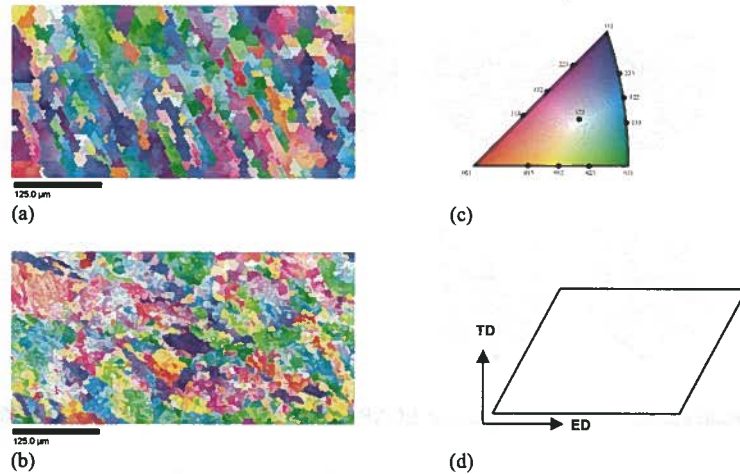


Fig. 5. EBSD patterns after 2nd ECAP pass of routes A (a) and C (b), respectively. The orientation triangle (c). Scheme of the cross-section of the sample used for all investigations (d)

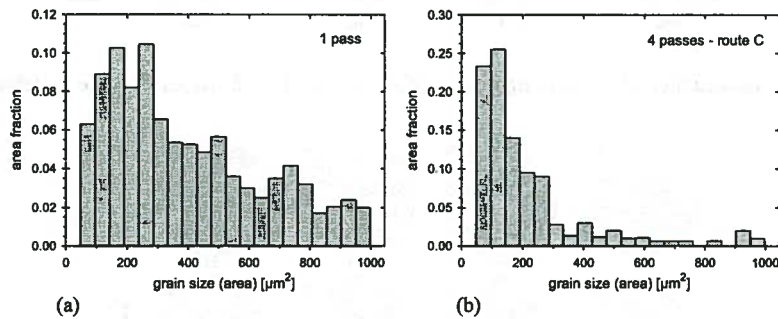


Fig. 6. The grain size distribution after one ECAP pass (a), and after 4 passes of route C (b) as determined from EBSD orientation maps

4. Discussion

Generally one can say that the texture evolution in the current investigation (a 120° tool) is not so strong and the amount of deformation per pass is much smaller when compared to ECAP deformation using a 90° tool. The quantitative analysis of the orientation distribution revealed three main texture components which develop quite rapidly after the first ECAP pass: $\{111\}\langle 011 \rangle$, $\{112\}\langle 011 \rangle$ and $\{110\}\langle 112 \rangle$ (*Brass*) where the first one is the most dominant. It seems reasonable since the $\{111\}\langle 011 \rangle$ and the $\{112\}\langle 011 \rangle$ components are ideal shear components. The third component $\{110\}\langle 112 \rangle$ is known as *Brass* orientation usually occurring in texture of rolled materials such as brass and austenitic stainless steel. All these fractions were determined with a tolerance of $\pm 5^\circ$ to the definite component orientation and did not grow when increasing the tolerance. This indicates a sharp texture.

The individuality of routes *A*, *B* and *C* is demonstrated in the evolution of the volume fraction of the three major components, what can be followed from Table.

For route *A* deformation the ideal shear component $\{111\}\langle 011\rangle$ is clearly dominating over the whole deformation range up to 7 passes or shear strain $\gamma = 6$. The *Brass* component $\{110\}\langle 112\rangle$ manifests similar tendency of changes in sense of the volume fraction, however, with ca. 3 times smaller amounts when compared to the $\{111\}\langle 011\rangle$ one.

Performing route *B* deformation up to 5 passes or $\gamma = 4.3$ again the $\{111\}\langle 011\rangle$ component remains clearly dominant followed by the other ideal shear texture component, whereas the *Brass* component becomes nearly negligible.

During deformation by route *C* up to 16 passes (shear strains $\gamma = 13.6$) the $\{111\}\langle 011\rangle$ as well as the *Brass* components dominate in the texture, but also the $\{112\}\langle 110\rangle$ shear component is quite strong having a volume fraction of 50 to 70% of the two others.

The character of the pole figures for the case of route *C* seems to confirm the 180-degree azimuthal rotation of texture of the processed Cu-billet about its longitudinal axis. The regularity is not so clearly observed in the case *B*. This rotation of the billet corresponds to a reversion of the shear direction. This can definitely be seen in the microstructure in Fig. 5. While the successive shearing with each during route *A* can be observed as elongation of the grains in Fig. 5a, route *C* deformation exhibits more equiaxial grain shape due to the opposite direction of the shear deformation when rotating the sample for 180° after each pass (Fig. 5b).

In spite of the above relations, some microstructure fragmentation with each pass proceeds also during route *C* deformation. Fig. 6 shows the grain size distribution after the initial pass and after 4 passes by route *C*. It can be seen in Fig. 6b that the gravity of the area fraction is shifted to smaller sizes (please note also the different in co-ordinate scales). This distribution presented in Fig. 6b is representative for deformation by all route types for higher strain. At lower strains the size distribution evolves somewhat different.

5. Summary

Development of texture during ECAP deformation has been described by $\{111\}\langle 011\rangle\{112\}\langle 011\rangle$ and $\{110\}\langle 112\rangle$ (*Brass*) components. In spite of deformation route (*A*, *B* or *C*) the $\{111\}\langle 011\rangle$ component is the strongest one. Together with the other ideal shear component, i.e. $\{112\}\langle 011\rangle$ it dominates in texture over the whole range of applied strain. The *Brass* component exists clearly during route *A* and quite strongly for route *C* deformation, while for route *B* it nearly vanishes. Observed regularities in changing the volume fractions of the main texture components for the routes *B* and *C* reflect the periodicity of sample orientation during the applied ECAP deformation.

The effects of macroscopic shearing the deformed material can be explicitly observed in the EBSD patterns. Route A exhibits elongated grain shapes, while for route C the initial equiaxial grain shape seems to be restored by the reversion of the shear direction.

Acknowledgements

The Science Foundation of Austria (FWF) is acknowledged for financial support under project P17095-N01.

REFERENCES

- [1] R.Z. Valiev, I.V. Islamgaliev, I.V. Alexandrov, *Progr. Mater. Sci.* **45**, 103 (2000).
- [2] H. Gleiter, *Progr. Mater. Sci.* **33**, 223 (1989).
- [3] Y. Iwahashi, Z. Horita, M. Nemoto, T.G. Langdon, *Acta Mater.* **46**, 3317 (1998).
- [4] M. Furukawa, Y. Iwahashi, Z. Horita, M. Nemoto, T.G. Langdon, *Mater. Sci. Eng. A* **257**, 328 (1998).
- [5] S.C. Vogel, I.J. Beyerlein, M.A.M. Bourke, C.N. Tomé, P. Rangaswamy, C. Xu, T.G. Langdon, *Mater. Sci. Forum* 408-412, 673-668 (2002).
- [6] R.D. Field, K.T. Hartwig, C.T. Necker, J.F. Bingert, S.R. Agnew, *Metal. Mater. Trans. A*, **33A** 965-972 (2002).
- [7] S.R. Agnew, U.F. Kocks, K.T. Hartwig, J.R. Weertman, *Proc. 19th Riso Int. Symp. Mater. Sci.*, Eds. J.V. Carstensen et al., Riso Nat. Lab., Roskilde, DK, 201-207 (1998).
- [8] S.R. Agnew, *Proc. 12th Conf. on Textures of Materials, Montreal, August 9-13* (Ed. J.A. Szipunar), 575-580 (1999).
- [9] J. Kuśnierz, *Mater. Sci. Forum* **426-432**, 2807-2812, (2003).
- [10] S.C. Vogel, D.J. Alexander, I.J. Beyerlein, M.A.M. Bourke, D.W. Brown, B. Clausen, C.N. Tomé, R.B. Von-Dreele, C. Xu, T.G. Langdon, *Mater. Sci. Forum* **426-432**, 2661-2666, (2003).
- [11] M.A. Gibbs, K.T. Hartwig, L.R. Cornwell, R.E. Goforth, E.A. Payzant, *Scripta Mater.* **39**, 1699-1704 (1998).
- [12] W.J. Kim, S.I. Hong, Y.S. Kim, S.H. Min, H.T. Jeong, J.D. Lee, *Acta Mater.* **51**, 3293-3307, (2003).
- [13] S.R. Agnew, J.A. Horton, T.M. Lillo, D.W. Brown, *Scripta Mater.* **50**, 377-381 (2004).
- [14] G.M. Stoica, S.R. Agnew, E.A. Payzant, D.A. Carpenter, L.J. Chen, P.K. Liaw, *TMS Proc. Ultrafine-Grained-Materials-3-Symposium*; Eds: Y.T. Zhu, T.G. Langdon, R.Z. Valiev, S.L. Semiatin, D.H. Shin, T.C. Lowe, 427-432. (2004).
- [15] W. Skrotzki, R. Tamm, R. Klemm, E. Thiele, C. Holste, H. Baum, *Mater. Sci. Forum* **408-412**, 667-472 (2002).

- [16] S.H. Yu, D.H. Shin, N.J. Park, M.Y. Huh, S.K. Hwang, *Mater. Sci. Forum* **408-412**, 661-666 (2002).
- [17] S.H. Yu, D.H. Shin, S.K. Hwang, *TMS Proc. Ultrafine-Grained-Materials-3-Symposium*; Eds: Y.T. Zhu, T.G. Langdon, R.Z. Valiev, S.L. Semiatin, D.H. Shin, T.C. Lowe, 227-234. (2004).
- [18] A. Vorhauer, diploma thesis, University of Leoben, Austria.

Received: 21 March 2005.